Structural and electronic properties of MgGe$_x$Sn$_{(1-x)}$N$_2$ semiconductors: The density functional theory investigation

K Kanchiang[1], T Cheiwchanchamnangij[2], S Pramchu[3], Y Laosiritaworn[3,4] and A P Jaroenjittichai[3,4]

[1] Program in Applied Physics, Faculty of Science, Maejo University, Chiang Mai 50290, Thailand
[2] Department of Physics, Faculty of Science, Mahidol University, Bangkok 10400, Thailand
[3] Department of Physics and Materials Science, Faculty of Science, Chiang Mai University, Chiang Mai 50200, Thailand
[4] Center of Excellence in Materials Science and Technology, Chiang Mai University, Chiang Mai, 50200, Thailand

The corresponding author's e-mail: atcharapunya@gmail.com

Abstract. In this work, we studied the lattice dynamics and electronic structures of nitride semiconductors MgGe$_x$Sn$_{(1-x)}$N$_2$, where x = 0, 0.25, 0.5, 0.75 and 1, using density functional theory (DFT) calculations. The core electronic states were represented via ultrasoft pseudo-potentials. From the results, lattice constants of MgGe$_x$Sn$_{(1-x)}$N$_2$ compounds decrease with increasing Ge concentrations according to the Vegard's law, where the lattice bowing coefficients p_a, p_b and p_c are 0.043, −0.019 and 0.087 Å respectively. For the electronic band structure, the N-p dominated valence band was found to shift down and IV-s dominated conduction band moves up with increasing the Ge concentrations. In addition, the energy gap bowing coefficients p_e is 0.916 eV.

1. Introduction

Wide-bandgap semiconductors such as group III-N have been used extensively as components of solid state lighting devices. For instance, AlN and GaN has been used to make ultraviolet LEDs [1] and blue LEDs [2], respectively. The alternative wide-bandgap semiconductors are crucial to search for more efficient optoelectronic devices and solar-energy conversion. Mixing of group-III elements in binary semiconductors (III-N), such as In$_x$Ga$_{(1-x)}$N, are considered to be a promising way in bandgap tuning. but the large lattice mismatch between InN and GaN produces phase separation in their alloys [3]. Thus, instead of binary compound semiconductors, the ternary compounds (II-IV-N$_2$) were proposed by replacing the group-III element with two elements of group-II and group-IV [4, 5]. For instance, ZnSn$_{1-x}$Ge$_x$N$_2$ was found synthesizable and it exhibits comparable properties in both lattice constants and bandgaps to those of InGaN. This shows a possibility to tune the bandgap from 2 eV to 3.1 eV by controlling of the Sn/Ge ratio [6]. In addition, the thermal stability of II-Ge-N$_2$ can be enhanced by replacing Zn with Mg [7]. Thus, in this research, two ternary semiconductors, MgGeN$_2$ and MgSnN$_2$, and the solid solutions of them, MgGe$_x$Sn$_{(1-x)}$N$_2$, were investigated using Density Functional Theory

(DFT) calculations with the HSE exchange-correlation functional as implemented in Quantum Espresso codes. This computational study will serve a fundamental knowledge for band structure and defect engineering of this new family of wide-bandgap semiconductors.

2. Materials and Methods

In this work, crystal structures and electronic structures of solid solutions, $MgGe_xSn_{(1-x)}N_2$ where $x = \{0, 0.25, 0.50, 0.75, 1\}$, were calculated based on density functional theory (DFT) provided in Quantum-Espresso package [8]. All valence electrons were included, while the core electronic states were represented via ultrasoft pseudo-potentials. The exchange correlation functional was projected with generalized gradient approximation (GGA) for structural relaxation. For the electronic band structure calculation, the hybrid functional approximation (HSE) with the mixing parameter of 0.5 were employed. The plane-wave cut-off energy was set to 80 Ry and the Monkhorst-Pack grid of 6×6×6 points was employed in the Brillouin zone. The atomic positions of orthorhombic structure in a space group $Pna2_1$ were used as the initial model structure [9], where unit cell consists of 16 atoms, i.e. 4 Mg atoms, 4 Sn atoms, and 8 N atoms. The bonding of Ge/Sn-N was considered in tetrahedral geometry, where 2×2×2 supercell was first generated and Sn/Ge ratio were chosen according to the x-fraction. Next, all atomic positions and lattice parameters were varied to minimize the total energy. The convergence was assumed achieving when the difference in total energies between the successive iterations being less than 10^{-4} Ry.

3. Results and Discussions

The calculated lattice parameters of $MgGeN_2$ and $MgSnN_2$ compounds are shown in table 1 and compared with the available experimental/theoretical values [5, 10-12]. As seen, lattice constants of $MgSnN_2$ are larger than that of $MgGeN_2$ because an ionic radius of Sn^{4+} (83 pm) is larger than that of Ge^{4+} (67 pm) [13]. For the $MgGe_xSn_{1-x}N_2$ compounds, the calculated lattice constants are shown in table 2. We found that the lattice constants of $MgGe_xSn_{1-x}N_2$ compounds decrease with increasing Ge concentration. The relations between lattice constants of solid solutions and those of ternary compound was found to follow Vegard's law [14] and can be expressed by a lattice bowing equation [15],

$$i_x = xi_{MgGeN_2} + (1-x)i_{MgSnN_2} - p_i x(1-x),$$

where i stands for lattice constants $\{a, b, c\}$, and p_i is the bowing parameters. From our results, the bowing coefficients p_a, p_b and p_c of $MgGe_xSn_{1-x}N_2$ are 0.043, −0.019 and 0.087 Å respectively.

Table 1. Lattice constants of $MgGeN_2$ and $MgSnN_2$ compounds in unit of Å.

Compound	Lattice constants	GGA	LDA[12]	GGA[13]	Exp.[14]
MgGeN$_2$	a	6.660	6.499	6.639	6.654
	b	5.546	5.389	5.540	5.518
	c	5.221	5.070	5.212	5.170
	E_g	5.120	3.010[15]	2.670	-
MgSnN$_2$	a	6.926	6.712	6.905	-
	b	5.948	5.746	5.932	-
	c	5.524	5.313	5.499	-
	E_g	3.327	-	1.160	-

Table 2. Lattice parameters of $MgGe_xSn_{1-x}N_2$ compounds in unit of Å.

Lattice constants	$MgGe_{0.25}Sn_{0.75}N_2$	$MgGe_{0.5}Sn_{0.5}N_2$	$MgGe_{0.75}Sn_{0.25}N_2$
a	6.873	6.812	6.735
b	5.854	5.766	5.653
c	5.446	5.343	5.294

Table 3. Bandgaps of $MgGe_xSn_{1-x}N_2$ compounds in unit of eV.

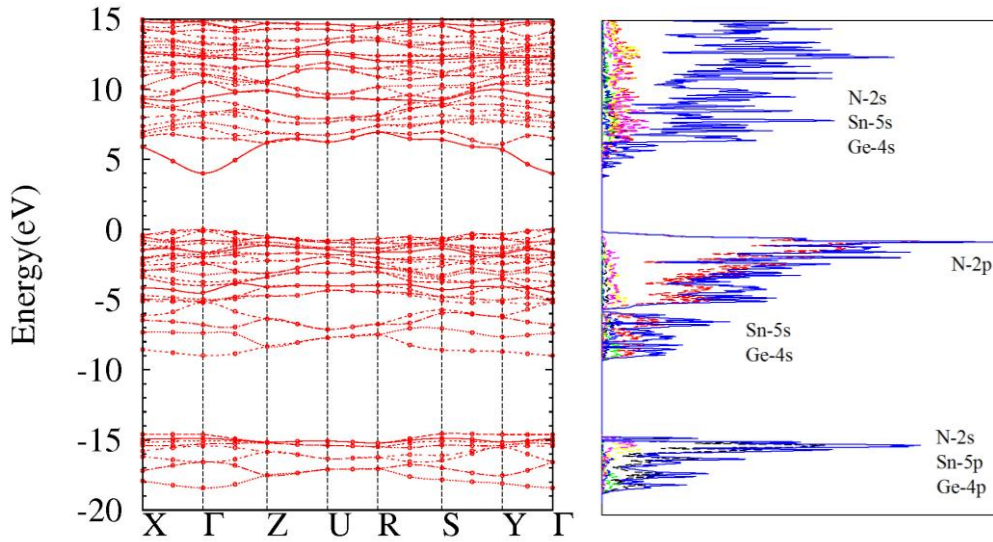| Compounds	$MgSnN_2$	$MgGe_{0.25}Sn_{0.75}N_2$	$MgGe_{0.5}Sn_{0.5}N_2$	$MgGe_{0.75}Sn_{0.25}N_2$	$MgGeN_2$
E_g	3.33 (3.43)[a]	3.60	4.00	4.50	5.12 (5.14)[a]

[a]QSGW gaps from Ref. [5]

Figure 1. Band structures, total DOS (blue line) and PDOS of $MgGe_{0.5}Sn_{0.5}N_2$compounds. N-2s, N2p, Ge-4s, Ge-4p, Sn-5s and Sn-5p are represented by black, red, green, yellow, dark blue and pink lines respectively.

The band structures and the partial density of states (PDOS) of $MgGe_xSn_{1-x}N_2$ compounds were calculated but only those of $MgGe_{0.5}Sn_{0.5}N_2$ are shown in figure 1 due to their similarity. From our band structure calculations, the valence band maximum (VBM) and the conduction band minimum (CBM) of all compounds are at Γ (0 0 0) point. The maximum valence band shifts down and the minimum conduction band shifts up with increasing Ge concentrations. This is consistent with the band alignment between $ZnSnN_2$ and $ZnGeN_2$ [16]. Note that, the band alignment between $MgSnN_2$ and $MgGeN_2$ has not been reported yet. The PDOS shows that the valence band from above –9 eV is mainly comprised of N-2p state. Moreover, in the energy range from –9 eV to –5 eV, PDOS also contains Ge-4s or Sn-5s according to the Ge/Sn ratio, which implies the presence of the bonding state, sp3-hybridization, in tetrahedral coordination of Ge-4s/Sn-5s and N-2p orbitals, while for the energy above -5 eV, it presents the p-p coupling state of Ge-4p/Sn-5p and N-2p. In addition, the bottom of the conduction band consists of N-2s state and Ge-4s state or Sn-5s state depending on the x-fraction, which implies the presence of antibonding state of Ge-4s/Sn-5s and N-2s orbitals. Besides, the energy

level of Sn-5s orbital lie*s* lower than that of Ge-4s orbital in the absolute scale. This s-s antibonding state then explains why the bandgap of MgGe$_x$Sn$_{1-x}$N$_2$ compounds increase with increasing Ge compositions. In addition, the s-s coupling state of the compounds with low *x*-fraction has higher energy due to their weaker bond. This can be described from considering the Ge-N bond length, which is shorter than Ge-N [5]. The bandgaps of MgGe$_x$Sn$_{1-x}$N$_2$ compounds also depend on the *x*-fraction as shown in table 3. Thus, we can write the bandgaps bowing equation [16] as

$$E_g^x = xE_g^{\text{MgGeN}_2} + (1-x)E_g^{\text{MgSnN}_2} - p_e x(1-x).$$

with the bandgap bowing coefficient p_e of 0.916 eV. From our results, the bandgap of MgGe$_x$Sn$_{1-x}$N$_2$ is tunable from 3.33 eV (MgSnN$_2$) to 5.12 eV (MgGeN$_2$) by controlling of the *x*-fraction. The parameter p_e is then an important parameter for designing the MgGe$_x$Sn$_{1-x}$N$_2$ solid solution with desired bandgap.

4. Conclusion

The crystal structure of ternary nitride semiconductors MgGe$_x$Sn$_{1-x}$N$_2$, where $x = \{0, 0.25, 0.50, 0.75, 1\}$ were calculated using the generalized gradient approximation (GGA). By comparing the atomic size of Ge and Sn, the lattice constants of the MgGe$_x$Sn$_{1-x}$N$_2$ compounds decrease with increasing Ge concentrations according to Vegard's law. The bowing coefficients p_a, p_b and p_c were found at 0.043, −0.019 and 0.087 Å respectively. For the electronic band calculation, the VBM of MgGe$_x$Sn$_{1-x}$N$_2$ was found dominated by N-2p orbitals, while the CBM composes mainly of the antibonding state of Ge-4s/Sn-5s and N-2s orbitals, depending on the *x*-fraction. Thus, the Ge/Sn ratio directly affects the bandgaps by altering the CBM. The bandgaps of MgGe$_x$Sn$_{1-x}$N$_2$ also follow Vegard's law with the bowing coefficient p_e of 0.916 eV. These bowing parameters (lattice constant and bandgap) are then important for optoelectronic design because they can be used to tune the bandgaps by varying the composition of the Ge/Sn, or to estimate the composition of a solution from the their associated lattice parameters.

References

[1]   Taniyasu Y, Kasu M and Makimoto T 2006 *Nature* **441** 325
[2]   Vurgaftman I and Meyer J R 2003 *J. Appl. Phys.* **94** 3675
[3]   Kuo Y-K, Liou B-T, Yen S-H and Chu H-Y 2004 *Opt. Commun.* **237** 363
[4]   Punya A, Lambrecht W R L and van Schilfgaarde M 2011 *Phys. Rev.* B **84** 165204
[5]   Jaroenjittichai A P and Lambrecht W R L 2016 *Phys. Rev.* B **94** 125201
[6]   Narang P, Chen S, Coronel Naomi C, Gul S, Yano J, Wang L W, Lewis Nathan S and Atwater Harry A 2013 *Adv. Mater.* **26** 1235
[7]   Punya Jaroenjittichai A 2016 *Integr. Ferroelectr.* **175** 186
[8]   Giannozzi P *et al.* 2017 *J. Phys. Condens. Matter* **29** 465901
[9]   Wintenberger M, Maunaye M and Laurent Y 1973 *Mater. Res. Bull.* **8** 1049
[10]   Arab F, Sahraoui F A, Haddadi K, Bouhemadou A and Louail L 2016 *Phase Transit*. **89** 480
[11]   Basalaev Y M, Demushin P V, Nikolaeva E V and Silinin A V 2011 *Mosc. Univ. Phys. Bull.* **66** 39
[12]   Basalaev Y M and Demushin P V 2010 *J. Struct. Chem.* **51** 1191
[13]   Shannon R 1976 *Acta Crystallogr.* A **32** 751
[14]   Denton A R and Ashcroft N W 1991 *Phys. Rev.* A **43** 3161
[15]   Osamura K, Naka S and Murakami Y 1975 *J. Appl. Phys.* **46** 3432
[16]   Punya A and Lambrecht W R L 2013 *Phys. Rev.* B **88** 075302